



A rain splash transport equation assimilating field and laboratory measurements

Thomas Dunne,^{1,2} Daniel V. Malmon,³ and Simon M. Mudd⁴

Received 4 March 2009; revised 13 July 2009; accepted 3 September 2009; published 7 January 2010.

[1] Process-based models of hillslope evolution require transport equations relating sediment flux to its major controls. An equation for rain splash transport in the absence of overland flow was constructed by modifying an approach developed by Reeve (1982) and parameterizing it with measurements from single-drop laboratory experiments and simulated rainfall on a grassland in East Africa. The equation relates rain splash to hillslope gradient, the median raindrop diameter of a storm, and ground cover density; the effect of soil texture on detachability can be incorporated from other published results. The spatial and temporal applicability of such an equation for rain splash transport in the absence of overland flow on uncultivated hillslopes can be estimated from hydrological calculations. The predicted transport is lower than landscape-averaged geologic erosion rates from Kenya but is large enough to modify short, slowly eroding natural hillslopes as well as microtopographic interrill surfaces between which overland flow transports the mobilized sediment.

Citation: Dunne, T., D. V. Malmon, and S. M. Mudd (2010), A rain splash transport equation assimilating field and laboratory measurements, *J. Geophys. Res.*, *115*, F01001, doi:10.1029/2009JF001302.

1. Models of Hillslope Evolution

[2] Hillslope evolution under transport-limited conditions is usually modeled as the result of one-dimensional sediment transport, represented by the mass balance equation

$$\frac{\partial z}{\partial t} = -\frac{1}{\rho_b} \frac{\partial Q_s}{\partial x} \quad (1)$$

where $\partial z/\partial t$ is the local rate of elevation change ($\text{m}^{-1} \text{a}^{-1}$), x is horizontal distance, ρ_b is the sediment bulk density (kg m^{-3}), and Q_s is the mass transport rate of sediment per unit width of hillslope ($\text{kg m}^{-1} \text{a}^{-1}$). Much of the work using equation (1) has been concerned with possible forms of equations for Q_s , and with the hillslope profiles such equations predict when subject to chosen boundary conditions [Culling, 1960; Hirano, 1969; Kirkby, 1971]. Ahnert [1976, 1987], Kirkby [1985, 1989], and Willgoose *et al.* [1991] incorporated the mass balance equation into numerical simulations of landscape evolution for a range of processes and boundary conditions such as base-level control.

[3] The theoretical work challenged geomorphologists to develop formulae relating sediment transport to its controls in order to quantify analyses of the geomorphic effects of climate, hydrology, vegetation, material properties, tectonism,

and time. Field and laboratory measurements of the sediment transport processes responsible for landform evolution have accumulated more slowly than the theoretical developments. They are necessary for understanding actual magnitudes and rates of geomorphic change, the relative roles and interactions of various processes, and the influence of environmental factors on rates of landform change and sediment production. Yet Dietrich *et al.* [2003] concluded that geomorphology has made little progress in developing process-based sediment transport equations for modeling landform evolution.

[4] Here we construct a transport equation for aerial rain splash, including particle creep along the surface, in the absence of overland flow. It is based on field experiments on grass-covered hillslopes in Kenya, laboratory experiments by us and others, and modification and generalization of a published model of particle trajectories. The equation is relevant to those events and portions of a landscape in which rain splash molds hillslopes, and, with some modification, to those parts of landscapes that contribute rain splash to rain flow transport [Moss *et al.*, 1979] in the form of interrill erosion [Meyer *et al.*, 1975].

[5] Rain splash transport is usually represented in equation (1) by an equation of the form

$$Q_s = \rho_b K \left| \frac{dz}{dx} \right|^b \quad (2)$$

In the most common applications of this equation b is assumed to be 1.0, leading to the combination of equations (1) and (2) into a topographic diffusion equation [Culling, 1960], and K represents the environmental factors that control transport intensity. This paper examines the functional form

¹Donald Bren School of Environmental Science and Management, University of California, Santa Barbara, California, USA.

²Department of Earth Science, University of California, Santa Barbara, California, USA.

³U.S. Geological Survey, Menlo Park, California, USA.

⁴School of Geosciences, University of Edinburgh, Edinburgh, UK.

of the transport equation for rain splash, but its main focus is quantification of the magnitude of sediment transport and the environmental factors that control K for this simplest of hillslope sediment transport processes.

2. Sediment Transport Equations for Rain Splash

[6] On intensively managed land surfaces, erosion by flowing water is prevalent, and although rain splash is the primary agent detaching soil, overland flow between and within rills is the dominant transport mechanism [Young and Wiersma, 1973; Moss *et al.*, 1979]. Hence, in agricultural engineering the role of raindrop impact has usually been incorporated into sediment transport equations for “interrill erosion,” which involves soil detachment by raindrops and transport by thin films of runoff [Meyer *et al.*, 1975; Foster, 1982; Lane *et al.*, 1992]. Experiments on these surfaces and on loose sediments in laboratories have shown that detachment and aerial transport by splash are affected by raindrop size, fall velocity, or kinetic energy; local gradient; surface cover; and various soil properties [Ellison, 1944b; Sreenivas *et al.*, 1947; Woodburn, 1948; Ekern, 1950; Morgan, 1978; Salles *et al.*, 2000; Van Dijk *et al.*, 2003]. Equations for sediment transport per unit contour width, were not usually developed from those studies.

[7] Geomorphologists have been interested in the morphogenetic role of rain splash under a wider range of environmental conditions, including natural landscapes where plant cover and soil structure limit overland flow, and thus where aerial rain splash transport may contribute significantly to hillslope erosion over long time periods. For example, on grass-covered, sandy soils of the western Congo, De Ploey and Savat [1968, p. 175] concluded that raindrop impact and “diffuse, discontinuous flow” were responsible for erosion, but hillslope evolution was essentially determined by splash. Mosley [1973] observed splash transport without runoff during an intense storm on convex badland divides in Wyoming, and conducted laboratory experiments to construct a rain splash transport equation with which he simulated the evolution of the convexities. Imeson [1977] and Kwaad [1977] demonstrated that rain splash (aerial and surface creep) was an important mechanism transporting stony loam colluvium down forested slopes in the Ardennes Mountains.

[8] Several geomorphologists have used rainfall simulators or single-drop formers and high-speed photography and videography in the laboratory to develop transport equations for single drop sizes, single particle sizes, and bare soil [De Ploey and Savat, 1968; Mosley, 1973; McCarthy, 1980; Poesen and Savat, 1981; Furbish *et al.*, 2007]. The present study extends this methodology to some of the complexities of natural hillslope surfaces and climates by incorporating the effects of plant cover and a distribution of raindrop sizes.

[9] Splash transport equations based on field measurements of mixed grain size soils would be more attractive but are problematic because of uncertainties in knowledge of natural rainfall and surface characteristics, the complicating influence of surface runoff, the variability of grain sizes, and the difficulty of making accurate measurements of splash transport in the field. However, Poesen [1986] measured splash transport of bare soils on cultivated, 14° – 23° slopes of by means of splash samplers and the resistance to splash

detachment with small splash cups. He found that the field-measured splash transport rates on bare sands and loams agreed well with those estimated from his laboratory-generated transport equation based on repacked soils, as did those from several other field studies of disturbed, bare soils.

[10] The status of sediment transport formulae for aerial rain splash can be summarized as follows. The functional form of the sediment transport equation for aerial rain splash is known approximately: transport is proportional to a power of gradient (b in equation (2)) lying between 0.6 and 1.1. However, the intensity of splash transport, represented by K in equation (2), for a given drop size and cover density is not easily predicted.

[11] The intensity of rain splash, measured as the amount of sediment detached from a smooth, bare surface by a unit of raindrop kinetic energy, drop size, or other index of erosivity has been widely measured. In the absence of high organic matter or other binding agent, detachability is related to median grain size, though not monotonically [Poesen and Savat, 1981]. For rainfall of uniform raindrop diameter the detachment rate per unit of kinetic energy was not linear for all soils [Poesen, 1985]. McCarthy [1980] showed that splashed mass was strongly related to both drop diameter and particle size in sands. Mosley’s [1973] laboratory experiments showed a sixfold increase in detachment over the range 0° – 25° , whereas field measurements by Froehlich and Slupik [1980, p. 95] indicated a two to threefold increase over 0° – 20° , and the laboratory experiments of McCarthy [1980, p. 106] and Furbish *et al.* [2007, Figure 9] revealed little or no effect of slope on detachment for loose sands. The only information on distances of splash [McCarthy, 1980; Poesen and Savat, 1981; Mouzai and Bouhadeb, 2003; Furbish *et al.*, 2007] also relates to smooth, bare surfaces. There is general agreement about the fractions of detached material that splash up and downslope on a bare surface [Poesen, 1985], although there appears to be a difference between sand and coarser particles [Mosley, 1973]. Furbish *et al.* [2007] provided a physical explanation for this fraction, based upon the upslope-downslope partitioning of drop momentum. Although detachment has been measured under various densities of plant cover [e.g., Ellison, 1948] and litter [e.g., Tsukamoto, 1966], quantitative relations between plant cover density and detachment have not been defined, it usually being assumed that splash occurs only from bare patches of soil. However, Furbish *et al.* [2009] have recently developed a model of the exchange of sand particles between shrub-stabilized mounds and the surrounding surface as a result of the spatial gradient of raindrop intensity around the center of the shrub.

3. Aims of the Study

[12] The study was designed with the following aims:

[13] 1. To measure rates of aerial rain splash transport under field conditions. The interaction of splash and overland flow was specifically avoided. Raindrop size, gradient, and grass cover density were varied between experiments on a single soil type.

[14] 2. To assimilate the resulting relations into a sediment transport equation for splash transport per rainstorm for the purposes of modeling hillslope evolution.

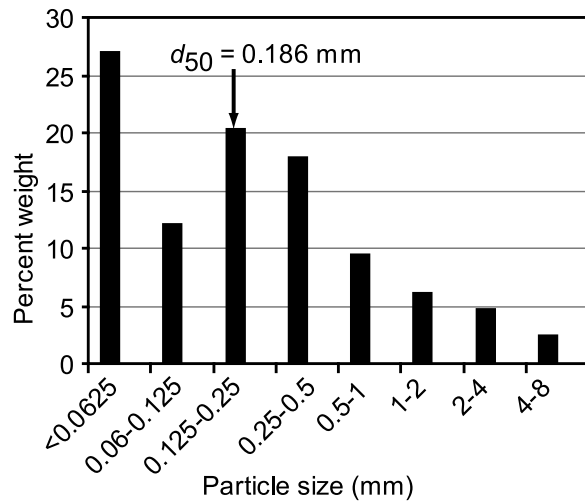


Figure 1. Texture of the surface 5 mm of soil, averaged from 14 samples scraped from the surface upslope and downslope of each splash collector before and after experiments on the seven plots. There was no consistent relationship between median (d_{50}) surface texture and either gradient or vegetation cover density, although plot 2 was significantly finer ($d_{50} = 0.06$ mm) than the other six plots, which had a mean d_{50} of $0.21 (\pm 0.05)$ mm.

[15] Our purpose is to develop a transport equation for the one-dimensional modeling of hillslope evolution over pre-human, morphogenetic time scales, which requires that parameterization of vegetation and rainfall effects be limited to features that can be estimated from coarse-grained paleo-environmental data. Also, we avoided agricultural soils, where tillage creates soil structures that evolve rapidly through crusting early in a rainstorm, which we have not observed in rainfall simulation experiments on more natural (though still grazed) clay/sand mixtures in Kenya grasslands. Although such effects have not been reported in other rain splash experiments, it is reasonable to anticipate that they might be important under some circumstances, particularly on bare, silt-rich soils.

4. Field Site

[16] Experiments were conducted on grassland at Eremito Ridge in Amboseli National Park, 150 km SE of Nairobi, Kenya [Dunne and Dietrich, 1980a]. The average gradient of the ridge is 0.02, with local variations of 0.012–0.12. The ridge is covered by a sandy clay loam with an organic content less than 1% and a bulk density of $1300\text{--}1600\text{ kg m}^{-3}$. The topsoil of the plots was poorly aggregated with a blocky, subangular structure and many fine pores. The surface layer (~ 5 mm deep) had an average grain size distribution illustrated in Figure 1. Sampling of the surface layer upslope and downslope of each splash sampler before and after the experiments indicated changes of only a few percent within any size class and no consistent coarsening or fining during the brief experiments. Although the surface contained $\sim 27\%$ of silt and clay, the only visible aggregates were of sand size. Infiltration capacity at a point varied between 1 and 8 cm h^{-1} with rainfall intensity and vegetation cover density [Dunne et al., 1991].

[17] Mean annual rainfall at the site is $\sim 25\text{--}30$ cm, concentrated in two seasons of 30–60 days duration separated by long dry seasons. The plant cover is clumped grass (*Aristida canadiensis*, *Chloris rioxburgiana*, *Sporobolus canadiensis*), grazed by wild herbivores and livestock. It varies seasonally and between years with rainfall and grazing pressure, and at the time of the experiments was 1–10 cm high with occasional stems rising to 20 cm. At the time of our experiments, during the dry season, small plots could be selected with cover densities ranging from 0.01 to 0.88.

5. Field Methods

[18] Three pairs of Ellison [1944a] splash samplers (Figure 2) were installed back-to-back, parallel to the contour beneath a rainfall simulator. The goal of the experiment was to measure the mass of sediment splashed across the front lips of the catch pans on the upslope and downslope sides of each sampler to yield a net mass flux per unit width of hillslope. The vertical board of the sampler between each pair of catch pans was 30 cm high and 15 cm wide. The samplers were different from the original design in one way. Ellison's [1944a] original sampler had a catch pan 1.25 cm wide in the slope-parallel direction and 9.5 cm deep, and with a lip that protruded 1.25 cm above the soil surface. To obtain as close a fit to the soil surface as possible, the lip of our catch pan was set at the ground surface, and to minimize breakage of the brittle topsoil during excavation, the catch pan depth was limited to 1 cm. Each catch pan was 10 cm long in the slope-parallel direction. Splashing of sediment from the soil across the sides of the pan was prevented by placing 8–10 cm high, porous bundles of thin sticks along the contour abutting the pan. Before each experiment, the pans were filled with water to prevent sediment from being splashed out of the pan. After rainfall, a wash bottle was used to sluice all particles from the 30 cm high vertical boards and the catch pans (which were removable from the assembly) into a storage bottle for filtering, drying, and weighing.

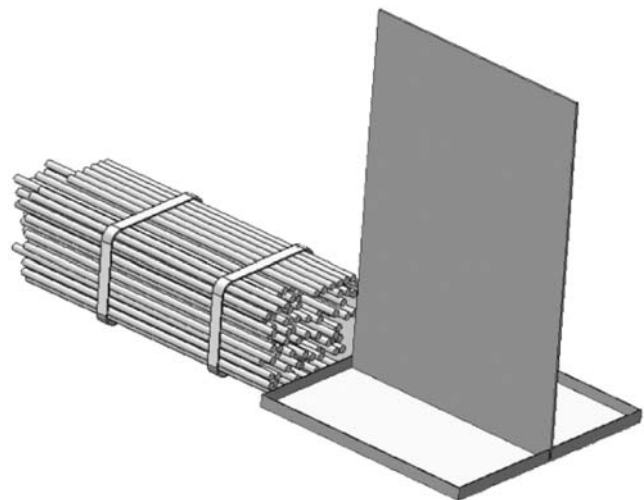


Figure 2. Ellison splash samplers placed back-to-back. Bundles of sticks provide a porous surface that prevents splashed soil from entering over the side of the catch pan. The bundle is shown on one side only for clarity.

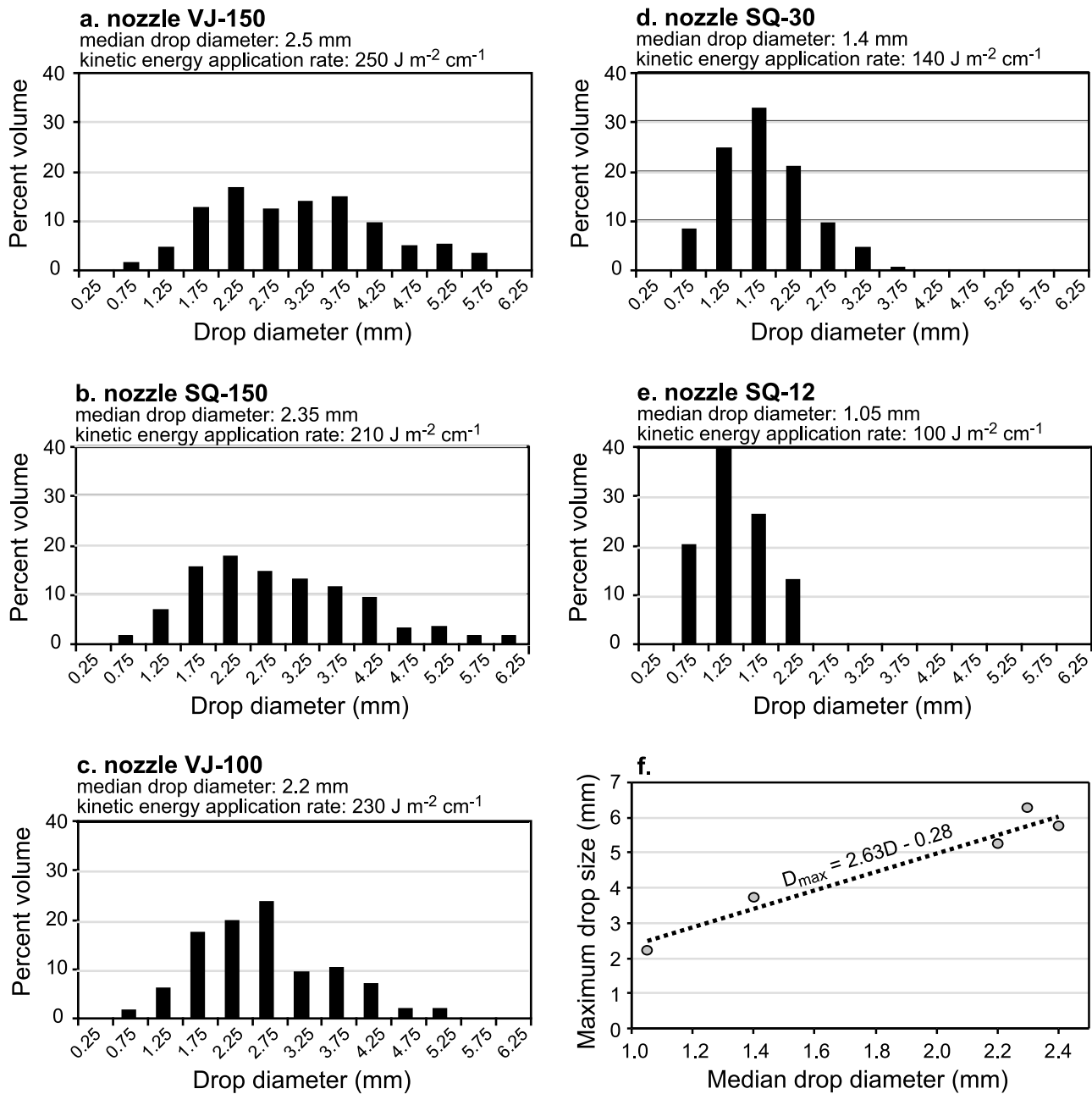


Figure 3. Frequency distributions of raindrop diameters generated by the five nozzles at an operating pressure of 115 kPa (except for SQ-150, which was calibrated and operated at 96 kPa). The nozzles were supplied by Spraying Systems Inc., Wheaton, Illinois, under the model numbers (a) Veejet H1/2U80150, (b) Fulljet 1/4HH80SQ150, (c) Veejet H1/2U80100, (d) Fulljet 1/2HH30WSQ, and (e) 1/4HH12SQ. (f) The relationship of the largest drop size to the median drop size generated by each nozzle.

[19] Artificial rain was generated with a simulator of the kind described by Dunne *et al.* [1980], with the nozzle 4.9 m above the ground, traveling along a 3 m long track at a speed of 0.7–0.9 m s⁻¹, so that the spray covered at least 50% of the plot at all times. Five nozzles of different sizes were used. Their drop size distributions and kinetic energy application, measured by the flour-pellet method [Carter *et al.*, 1974], are shown in Figure 3. An artificial rainstorm from each nozzle is referred to by the median drop size representing the distributions shown in Figure 3: 2.5 mm, 2.35 mm, 2.2 mm,

1.4 mm, and 1.05 mm. Rain distribution was measured with networks of twelve 10 cm diameter gauges around the three replicate pairs of samplers, and isohyetal maps were drawn for each experiment for interpolation of the rain falling within 0.25 m of each catch pan lip. Most experiments involved the application of only 5 to 20 mm of rain, and with the wisdom of hindsight it would have been preferable to increase the size of splashed sediment samples by using longer applications. Concern about altering the surface texture of the soil limited the amounts of rain applied, but sampling the texture imme-

Table 1. Plot Characteristics

Plot	Gradient	Cover
1	0.035	0.01
2	0.017	0.31
2c ^a	0.017	0.16
3	0.012	0.88
3c ^a	0.012	0.60
4	0.068	0.08
5	0.119	0.01
6	0.036	0.16
7	0.040	0.08

^aThe c designations for plots 2 and 3 refer to clipping to reduce ground cover after a sequence of experiments with each of the nozzles.

diately adjacent to the pans before and after each set of experiments revealed no measurable changes in texture and there was no visible change in surface condition.

[20] The plot surface was closely observed during each application. At the first sign of the surface glistening from water accumulation, the nozzle was abruptly pulled to one end of the plot and the spray was interrupted and restarted after the surface had drained. In this way, we avoided interaction of raindrop impact with a surface water film, although we had no precise control over the moisture content of the surface soil. There was no sign of water repellency at the soil surface or of aggregate breakdown as the surface soil was not aggregated at a visible scale.

[21] Seven plots were used for the measurements (Table 1), and on two of them (2 and 3) plant cover was reduced by clipping before some rainfall applications (measurements after clipping are indicated by “c” in Table 1). Plant cover density, including litter which provided only a small fraction of the cover, was measured as the average of visual estimates by two to four observers with the aid of a 0.5 m square quadrat sampler placed immediately upslope and downslope of each catch pan [Greig-Smith, 1983]. Standard errors among observers and quadrats averaged 4.7% of the mean cover density for each plot. The local gradient over 0.5 m intervals upslope and downslope of each splash sampler was measured with an engineering level. The experiments included variations in raindrop size, local gradient, and plant cover density on a single soil type, but only a limited set of combinations of gradient and cover could be found in the vicinity.

[22] Composite samples of the upper 5 mm of soil on each plot were collected for wet sieve analysis before and after each set of experiments, and 33 composite samples of splashed sediment from individual rainfall applications were saved for grain size analysis in a settling tube.

6. Analysis of Splash Measurements

[23] The mass of sediment caught in each pan represented a flux through a 15 cm wide length of contour passing through the outer lip of the catch pan as a result of a certain number of raindrop impacts within splashing range of the pan (5–10 cm by observation and calculation). The amount of sediment splashed by a fixed distribution of drop sizes should increase linearly with the number of drops, and therefore with the depth of rainfall in the absence of interactions between the impacts and in the absence of a water film. Nonlinear relationships between rainfall intensity and the amount or rate of soil splash, such as those reported by Ellison [1944b,

p. 181] and Gilley and Finkner [1985, p.144] presumably result from relationships between intensity and drop size, limitations on the detachment rate due to cohesion, or surface water accumulation. These effects were minimized in our study. Thus, for each nozzle the mass of sediment passing through the 15 cm width was divided by the depth of rain falling immediately upslope or downslope of the catch pan, and the splash transport was expressed in units of kg per meter of contour per cm of rain.

[24] When the splash was plotted against local hillslope gradient upslope or downslope of each pan, the results confirmed our visual observations that extremely local (1–10 cm scale) variations in vegetation patchiness and microtopography obscured any such relationship, given the narrow range of gradient (0.012–0.12) that could be sampled at the field site. Therefore, we combined all measured splash values, regardless of upslope or downslope direction, into an analysis of the effects of raindrop characteristics and vegetation cover on the mass splashed, essentially treating all of the gradients as zero. Thus, our field results relate only to the magnitude, $\rho_b K$, of the fluxes in equation (2), and we developed a theoretical slope function for partitioning transport upslope and downslope on gradients steeper than the measurement sites (see later).

[25] We tested the hypothesis that the mass of sediment splashed across a unit width of contour (regardless of direction) is a function of median raindrop diameter and ground cover density (Figure 4). For each drop size distribution, mass splashed declines exponentially as cover density (C) increases at rates that are inversely correlated with the median raindrop diameter (D). Although responses to the three larger drop sizes are roughly the same, the effectiveness of small drops diminishes faster than that of large drops, which can strike the surface with little change of momentum as they pass through the ground cover. Longer splash trajectories resulting from large drops with higher impact velocities may also be preferentially reduced by vegetation. The mass splashed decreases with increasing cover much faster than the commonly assumed linear relationship to $(1 - C)$, presumably because the density of erect plant stems and of vegetation patches correlates with the measured areal cover fraction and is responsible for filtering sediment out of the lateral splash trajectories. Multiple regression analysis yielded

$$M_0 = aD^j e^{fC/D} \quad (3)$$

($R^2 = 0.80$, $n = 33$, $p < 10^{-11}$) where M_0 is mass of soil splashed across a contour on a horizontal surface ($\text{kg m contour}^{-1} \text{ cm rain}^{-1}$); D is median drop diameter (mm); C is cover density (decimal fraction); and a (0.0104), j (0.927), and f (–10.28) are parameters related to the detachability of this soil. Including hillslope gradient in the regression did not improve the result significantly, possibly because of the limited range of gradients (0.012–0.12) in the study area. Transport depends on both mobilization (M_0) and distance of travel, as shown in section 7.2.2, where we use equation (3) to parameterize a transport equation.

[26] Almost all of the surface particles could be mobilized by the raindrop distributions applied. Particle sizes of the splashed soil ranged from <0.062 mm to 2.8 mm and

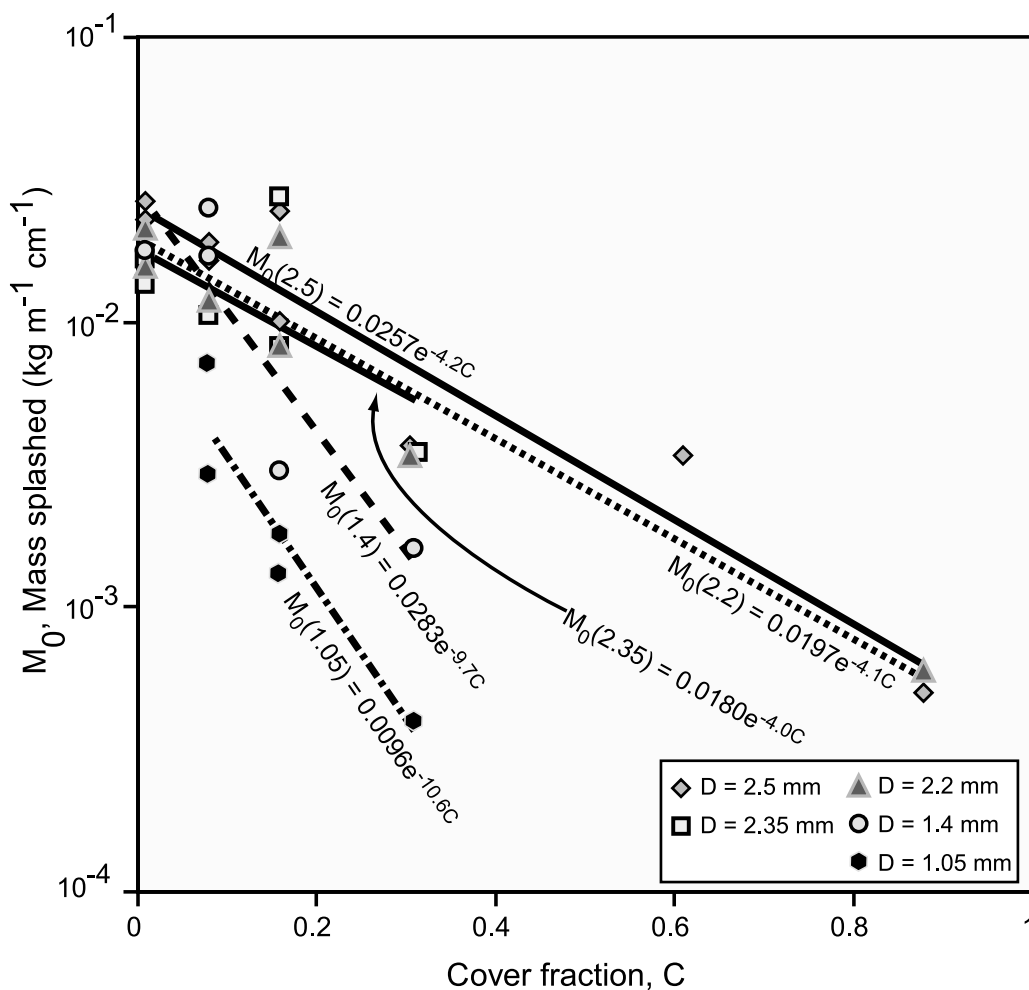


Figure 4. Rain splash transport ($\text{kg m}^{-1} \text{cm}^{-1}$ of rain) plotted against ground cover fraction (C) for artificial rainstorms with indicated median drop diameters (D). Sample sizes and p values are $n = 9, p < 10^{-4}$ for $D = 2.5$ mm; $n = 6, p < 0.16$ for $D = 2.35$ mm; $n = 8, p < 10^{-3}$ for $D = 2.2$ mm; $n = 5, p < 0.05$ for $D = 1.4$ mm; $n = 5, p < 0.05$ for $D = 1.05$ mm.

involved a selection from the surface texture (Figure 5). The silt and clay on the soil surface provided little cohesion: enough for some particles to travel together as millimeter-sized aggregates, but no cohesive surface was exposed. Thus,

any threshold drop diameter or momentum required for transport of the silt and clay particles was small. A slight extrapolation of *McCarthy's* [1980] measurements of critical drop sizes for a range of sand sizes (Figure 6) suggests that

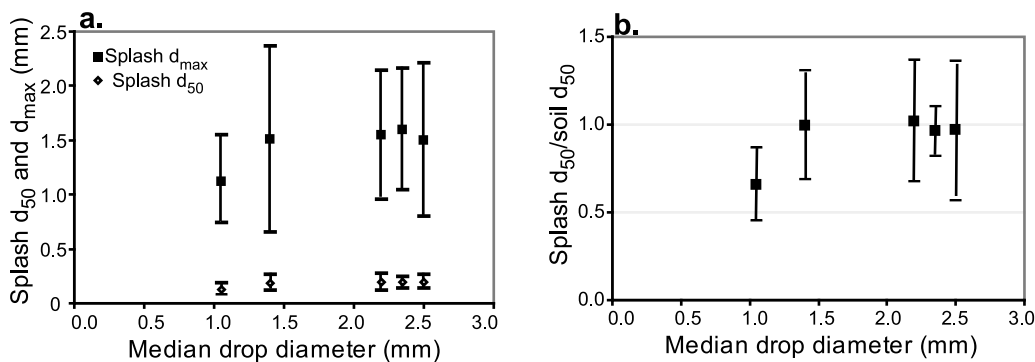


Figure 5. Selectivity of particle sizes by splash in artificial rainstorms with five nominal median raindrop sizes on the field plots in Kenya. (a) Average (\pm standard deviation) of median (diamonds) and maximum (squares) particle sizes splashed. (b) Average (\pm standard deviation) ratio of median particle of splashed material to median particle size of surface soil.

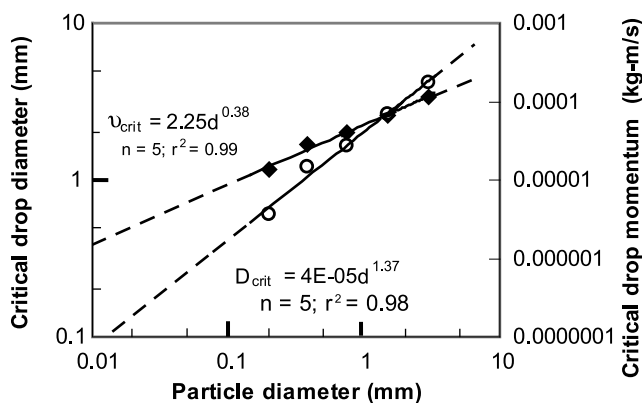


Figure 6. Critical drop sizes and critical drop momentum required to splash loose sediments with various particle sizes. The data are calculated from laboratory measurements by McCarthy [1980] and for the smallest particle size (0.2 mm) by Ekern and Muckenhirn [1947]. Dashed lines are projections of the best fit regression equations (solid lines) over the range of interest in our field experiments.

even the smallest median raindrop size in our experiments was large enough to mobilize approximately one half of the surface particles. The silt and clay particles, which constituted 15–52% of the plot surfaces, entered the splash in copious amounts, making each splash crown opaque. The d_{50} grain sizes for splashed material (Figure 5a) averaged 0.12 (standard deviation ± 0.05) mm for the 1.05 mm median drop diameter and 0.19 (standard deviation ± 0.06) mm for the others, essentially the same size as the median of the surface. The maximum particle size splashed into a sampler ranged from 0.42 to 1.18 mm (averaging 1.1 mm) for 1.05 mm storms and from 0.59 to 2.4 mm (averaging 1.5 mm) for the other drop sizes, with no apparent trend. The maximum drop sizes produced by our sprinklers (Figure 3f) ranged from 2.25 mm to 6.25 mm, and according to McCarthy's laboratory results (Figure 6) should be competent to splash particles of 1.07 mm and >8 mm, respectively, for the smallest and largest nozzles.

7. Generalization of a Transport Model

7.1. Instantaneous Rain Splash Rate

[27] We derive a model for the instantaneous rain splash transport (q_{inst} , $\text{kg m}^{-1} \text{cm}^{-1}$), as a function of cover density, drop size, and hillslope gradient, which can be calibrated with the field data described above, and incorporated into equation (2). We emphasize from the outset the above mentioned differences between the field conditions and laboratory conditions for which theoretical models have been formulated and calibrated. Theoretical [e.g., Furbish et al., 2007] and experimental [e.g., De Ploey and Savat, 1968; Mosley, 1973; McCarthy, 1980; Poesen, 1985; Mouzai and Bouhadef, 2003; Furbish et al., 2007] analyses of rain splash use single (usually large) drop sizes and single (usually sand) grain sizes. Field experiments on natural soils involve a wide range of drop sizes (~ 25 -fold in Figure 3) and an even wider range of grain sizes (~ 100 -fold in Figure 1), ranging in this case from clay to coarse sand. Another difference between laboratory conditions and our field plots was that surface

cratering in the field was observed to be less pronounced than is routinely described in laboratory experiments because the sand grains in the natural soil were mixed with finer particles and appeared to the eye and touch to be more densely packed.

[28] Current models of splash transport analyze the splash and creep process in terms of either the alongslope dispersal of drop momentum creating a measured exponential distribution of particle travel distances [Mouzai and Bouhadef, 2003; Furbish et al., 2007] or a distribution of particle takeoff speeds and angles from which travel distances are calculated [De Ploey and Savat, 1968; McCarthy, 1980]. These two approaches have not yet been reconciled formally, but because the Furbish et al. [2007] method has only been calibrated for uniform sands and requires the identification of a critical drop momentum from the available data on sand, we have used the second approach. However, we did not combine the distributions of takeoff angle and speed to derive the expected distribution of splash distances on a slope. Instead we have used average values estimated from earlier laboratory measurements, as described below. The approach is a compromise similar to the use of an average infiltration capacity in a runoff calculation to represent what is known to be a variable with a probability distribution.

[29] The first component of the model is an estimate of the fraction of sediment mass (F) splashed downslope by a single raindrop impact on a slope of angle β . This fraction has been measured in laboratory experiments on a range of gradients and summarized by McCarthy [1980] and Poesen [1985], who related the fraction to an exponential function of β . Our fit to the available data (Figure 7) yields the equation

$$F = 1 - 0.5e^{-2.2 \tan \beta} \quad (4a)$$

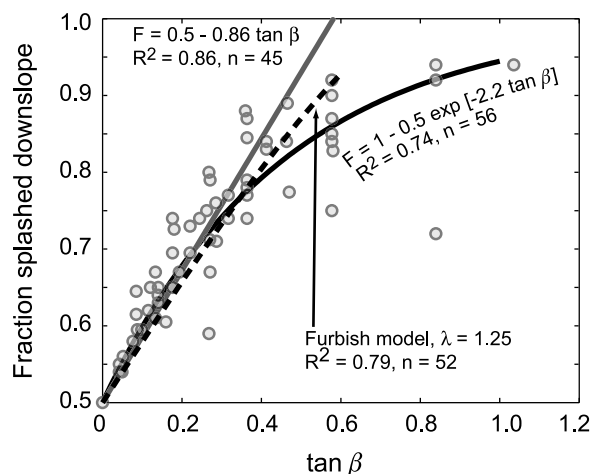


Figure 7. Fraction of sediment splashed downslope in laboratory experiments compiled by De Ploey and Savat [1968], McCarthy [1980], and Poesen [1985]. The linear regression was fitted to the measurements over the range $0 < \beta \leq 25^\circ$. The curve was fitted to the entire data set with the form $F = 1 - 0.5e^{-2.2 \tan \beta}$. Regression coefficients for single size sands were slightly sensitive to grain size; for 0.1 mm sand the coefficient in the exponent was -2.45 and for 0.59 mm sand was -3.13 (data from Poesen [1985]). All regressions were constrained to fit the point (0, 0.5).

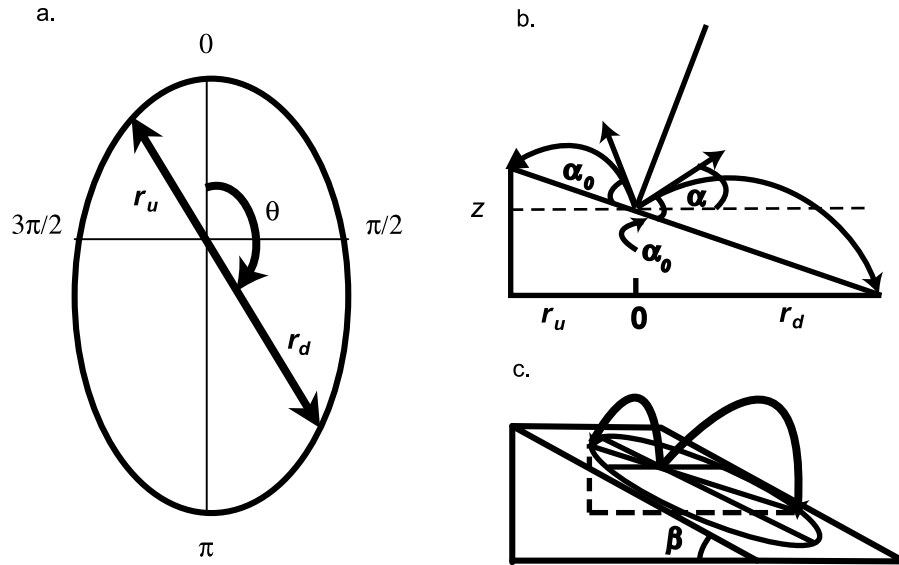


Figure 8. Geometry and definition of symbols for the trajectory of soil particles ejected by a raindrop impact on a plane. (a) Range line (horizontal projection); (b) definition of α_0 ; (c) distances of travel varying with direction, θ , before impacting the plane.

Figure 7 also shows that for $\beta < 25^\circ$ ($\tan \beta < 0.47$), where fine-textured soils are likely to survive under sparse vegetation, the fraction varies linearly with gradient

$$F = 0.5 + 0.86 \tan \beta \quad (4b)$$

Since these data were obtained from drops with a range of size and impact speed, we are interpreting that the fractions are stable for each raindrop that impacts the ground between plants or litter.

[30] Based on high-speed imaging, *Furbish et al.* [2007] suggested a physical basis for this partitioning. Upon raindrop impact, momentum transferred to the sediment is partitioned between radial and downslope components. They proposed that this partitioning is linearly proportional to hillslope gradient (i.e., the ratio of downslope momentum to radial momentum is equal to $\lambda \tan \beta$ where λ is an empirical partitioning coefficient). We derive the fraction splashed downslope based on equation (8) of the *Furbish et al.* [2007] model, which describes the probability of mass splashed as a function of radial distance from the point of impact, r , and direction, θ ($\theta = \pi$ is directly downslope); the probability, integrated over r and θ , is equal to unity by definition. Inserting a momentum partitioning of $\lambda \tan \beta$ into the *Furbish et al.* [2007] model and integrating over r and from $\theta = \pi/2$ to $\theta = 3\pi/2$ yields the fraction splashed downslope:

$$F = \frac{1}{2} + \frac{\lambda \tan(\beta)}{\pi} \sqrt{1 - \lambda^2 \tan(\beta)^2} + \frac{1}{\pi} \text{ArcTan} \left(\frac{\lambda \tan(\beta)}{\sqrt{1 - \lambda^2 \tan(\beta)^2}} \right) \quad (5)$$

The value of λ that best fits the measured F values summarized by *Poesen* [1985] for $\beta < 25^\circ$ is 1.25 (Figure 7).

[31] The second component of our model, which calculates the net travel distance of all particles resulting from a drop

impact on a sloping plane (Figure 8), modifies an approach presented by *Reeve* [1982]. *Reeve* proposed that a raindrop splashes a mass of grains, m , radially around its impact point. He assumed that particle ejection was symmetrical about the vertical, whereas high-speed videography by *Furbish et al.* [2007] recorded differences between the slope-parallel components of launch speeds. By contrast, high-speed photography [*McCarthy*, 1980] and laboratory studies of radioactively tagged particles by *De Ploey and Savat* [1968] indicated that ejection occurred almost symmetrically about the surface normal (Figure 9), suggesting that in the early stage of the impact the force from the pressure wave in the drop recoiling from the surface is much larger than the force of gravity. This seems even more likely at our field site where soil was more densely packed and the permeability was lower (by a factor of $\sim 10^{-3}$) than in the laboratory sand, and the observed craters were shallower than those described in the laboratory [*McCarthy*, 1980; *Furbish et al.*, 2007].

[32] Even if the splash is approximately symmetrical around the surface normal, however, the asymmetry of mass transport represented by F indicates that the proportions of the drop and mobilized sediment that travel downslope from the point of impact must vary with the gradient. Improvements in observational technology are still needed to resolve these differences, but the quantitative implications for our model are minor, and we have used the approximation suggested by *De Ploey and Savat* [1968] and *McCarthy* [1980]. High-speed photographs [*McCarthy*, 1980] and the distribution of grains after each impact [*McCarthy*, 1980; *Furbish et al.*, 2007] indicate that local velocity variations in the splash tear the fluid crown apart and deposit grains at various distances from the impact area, but since we cannot measure the distribution of such distances for the disparate particle sizes in the field soil, we express their trajectories in terms of average takeoff speeds and angles.

[33] The takeoff angle when the plane is horizontal ($\beta = 0^\circ$) is the critical takeoff angle relative to the plane itself, α_0 in Figure 8. In the model, particles launched at the average angle

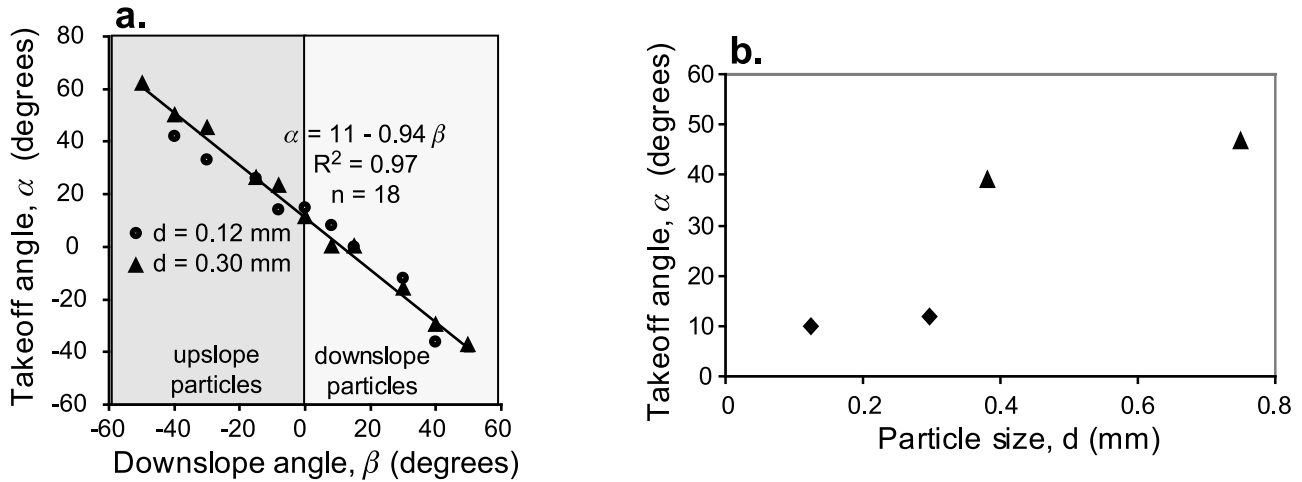


Figure 9. (a) Takeoff angles relative to the horizontal (α in Figure 8b) for upslope and downslope transport by single raindrops on a surface set at various angles. Two sets of particles (0.12 mm (circles) and 0.30 mm (triangles)) were used for the experiments by *De Ploey and Savat* [1968], but their regression equations were almost identical. Proximity of the two regression coefficients to -1.0 indicates that both upslope and downslope takeoff angles change at the same rate as the hillslope angle (β), though in opposite directions, revealing that the ejection is approximately symmetrical about the surface normal. The regression equation for the combined data sets is $\alpha = 11 - 0.94\beta$; $r^2 = 0.97$, $n = 18$. However, as the slope is close to 1.0 , the line is constrained to have a slope of unity without any significant change in the sum of squares of the minimized residuals. Here α_0 is the value of α when $\beta = 0^\circ$, in this case 11° . (b) Takeoff angles for four soil textures measured (using differing methodologies) by *De Ploey and Savat* [1968] (diamonds) and *McCarthy* [1980] (triangles).

and speed come to rest where their trajectories intersect the ground surface, and do not rebound upon contact with the slope. Our close field observations confirmed the lack of rebound. *Reeve* [1982] derived an expression for the “range line,” the horizontal projection of the closed curve, $r(\theta)$, representing the termini of all the particles splashed by a raindrop on a plane of slope angle β (Figures 8a and 8c), where r is the radial distance of splash and θ is the direction in cylindrical coordinates, taken as zero in the upslope direction and increasing clockwise. This range line is a notional one, reflecting the average distances that would be traveled by particles with the average takeoff speed v_t and angle, α_0 .

[34] Like *Reeve* [1982], we solve the ballistic trajectory of splashed sediment particles by the application of Newton’s second law in three dimensions. The resulting range line differs from that of *Reeve* [1982] because we use the surface normal as the axis of symmetry of the splash. Our derivation of the range line is

$$r = \frac{v_t^2 \left(2 \cos \theta \sec \beta \sin \alpha_0 \tan \beta + \sqrt{2} \sqrt{1 + \cos(2\alpha_0) \sec^2 \beta + \cos(2\theta) \tan^2 \beta} \right)}{g(\cos^2 \theta \sec^2 \beta + \sin^2 \theta) \cos \beta \cos \alpha_0} \quad (6)$$

[35] *Reeve* [1982] showed that the upslope flux of sediment (s_{up}) across a length L of hillslope contour per unit of rainfall is

$$s_{up} = \frac{imL}{2\pi} \int_{\pi/2}^{\pi} r \cos \theta d\theta \quad (7)$$

and the downslope flux (s_d) is

$$s_d = -\frac{imL}{2\pi} \int_{\pi/2}^{3\pi/2} r \cos \theta d\theta \quad (8)$$

where i represents the number of raindrops per unit rainfall depth per unit area and m is the mass splashed by each drop. Each integral contains the area in the horizontal plane that lies within splash range, $r(\theta)$, of the unit length of contour (or collector) and therefore also indicates the volume of water that falls onto that area in a rainfall of unit depth. The net downslope transport per unit of contour length results from the difference between equations (7) and (8):

$$q_{inst} = \frac{s_d - s_u}{L} \quad (9)$$

[36] In our analysis the flux is weighted by the proportions of mass splashed up and downslope according to equation (4) or (5). The available data on slope-wise partitioning of the splashed mass do not allow the splashed fraction to be specified as a function of θ and incorporated directly into the integrals of equations (7) and (8). Instead, we make the

approximation of distributing the upslope and downslope fractions as averages in each direction. Thus, the net downslope flux per unit width of contour and per unit of rainfall becomes

$$q_{inst} = \frac{Fs_d - (1-F)s_u}{L} = -\frac{im}{2\pi} \left[F \int_{\pi/2}^{3\pi/2} r \cos \theta d\theta + (1-F) \int_{-\pi/2}^{\pi/2} r \cos \theta d\theta \right] \quad (10)$$

We parameterized equation (10) by obtaining im from laboratory measurements and our field data as described below.

7.2. Model Parameterization

7.2.1. Values From Laboratory Measurements

[37] Equation (6) requires a mean takeoff angle, α_0 , for which the available data are sparse. In Figure 9a we plotted takeoff angles relative to the horizontal (α in Figure 8b) of sediment splashed directly up and downslopes of various angles, as measured in the laboratory by *De Ploey and Savat* [1968, Table 2], to derive α_0 . Figure 9a summarizes our analysis of the data, which indicate a value of $\alpha_0 = 11^\circ$ for the

which $\beta = 0$, $F = 0.5$, and evaluation of the integral yields the mass splashed in one direction per unit length of contour per unit depth of rainfall, M_0 :

$$M_0 = \frac{imv_t^2 \sqrt{2} \sqrt{1 + \cos 2\alpha_0} \sin \alpha_0}{2\pi g} \quad (12)$$

M_0 is the quantity that was measured in the field experiments under a range of drop size (D) and cover density (C). Combining equation (3), which summarizes the field results, with equation (12) yields

$$im = \frac{2\pi g a D^j e^{fC/D}}{v_t^2 \sqrt{2} \sqrt{1 + 2 \cos \alpha_0} \sin \alpha_0} \quad (13)$$

which can be substituted into equation (10) to yield

$$q_{inst} = -\frac{a D^j e^{fC/D}}{\sqrt{2} \sqrt{1 + 2 \cos \alpha_0}} \cdot \left[F \int_{\pi/2}^{3\pi/2} \Omega(\theta) \cos \theta d\theta + (1-F) \int_{-\pi/2}^{\pi/2} \Omega(\theta) \cos \theta d\theta \right] \quad (14a)$$

where

$$\Omega(\theta) = \frac{(2 \cos \theta \sec \beta \sin \alpha_0 \tan \beta + \sqrt{2} \sqrt{1 + \cos(2\alpha_0)} \sec^2 \beta + \cos(2\theta) \tan^2 \beta)}{(\cos^2 \theta \sec^2 \beta + \sin^2 \theta) \cos \beta} \quad (14b)$$

particle sizes used in the experiments (0.088–0.177 mm and 0.25–0.35 mm). Figure 9b summarizes the available data on takeoff angles for various particle sizes, which suggest a positive relationship between takeoff angle and particle size. Since the soil in our experiments was generally finer than those used for the laboratory measurements, we chose from Figure 9b an average takeoff angle of 10° . *De Ploey and Savat* [1968] published takeoff speeds of 2 m s^{-1} for fine sands, and *McCarthy's* [1980] measurements averaged 1.5 m s^{-1} and 1.4 m s^{-1} , respectively, for 0.38 mm and 0.75 mm sands. However, the need to specify a takeoff speed can be obviated through calibration against field data, as we will demonstrate.

7.2.2. Values From Field Measurements

[38] Equation (10) now contains a single unknown expression, im , the mass of sediment splashed per unit area per unit depth of rainfall, which we determine from our field measurements, summarized in equation (3), in the following way. From equation (10), the mass splashed per unit length of contour and per unit depth of rainfall in the downslope direction on a slope of β is

$$M_\beta = -F \frac{im}{2\pi} \int_{\pi/2}^{3\pi/2} r \cos \theta d\theta \quad (11)$$

Substitution of equation (6) into equation (11), application to a horizontal plane, similar to the field measurements, for

Cancellation of v_t^2 between equations (6), (11), and (13) removes the need for an independently specified takeoff speed.

8. Model Results

[39] Equation (14) is the final splash transport equation, calibrated by equation (13), in which uncertainties introduced by the distribution of the takeoff angle and the alongslope partitioning of drop and sediment momentum are combined with other uncertainties from the field experiments. Figure 10 shows sample calculations for two median drop sizes and a range of cover densities and hillslope gradients to indicate (1) the form of the relationship between transport and gradient and (2) how the effects of drop size and cover density interact. The form of the slope function is determined by the partitioning function, F . If the fraction is estimated over the full range of the experimental data (Figure 7 and equation (4a)), the predicted splash transport varies with $\tan^{0.78} \beta$, equivalent to a value of $b = 0.78$ in equation (2) (Figures 10c and 10d). The equation yields values of $0.0005\text{--}0.0015 \text{ kg m}^{-1} \text{ cm}^{-1}$ of rain, respectively, for bare slopes of 10° ($\tan \beta = 0.176$) and median raindrop sizes of 1–3 mm, and $0.0000002\text{--}0.0005 \text{ kg m}^{-1} \text{ cm}^{-1}$ of the same raindrop sizes, respectively, for cover densities of 1.0 on the same slope. If the estimation of F and the application of equation (14) are limited to slope angles $<25^\circ$, flux varies linearly with $\tan \beta$ (Figures 10a and 10b).

[40] If there were no downslope partitioning of the splash itself, according to equation (4a), the difference between the unweighted integrals in equation (14) would be almost exactly a linear function of $\tan \beta$. Thus, it is the effect of

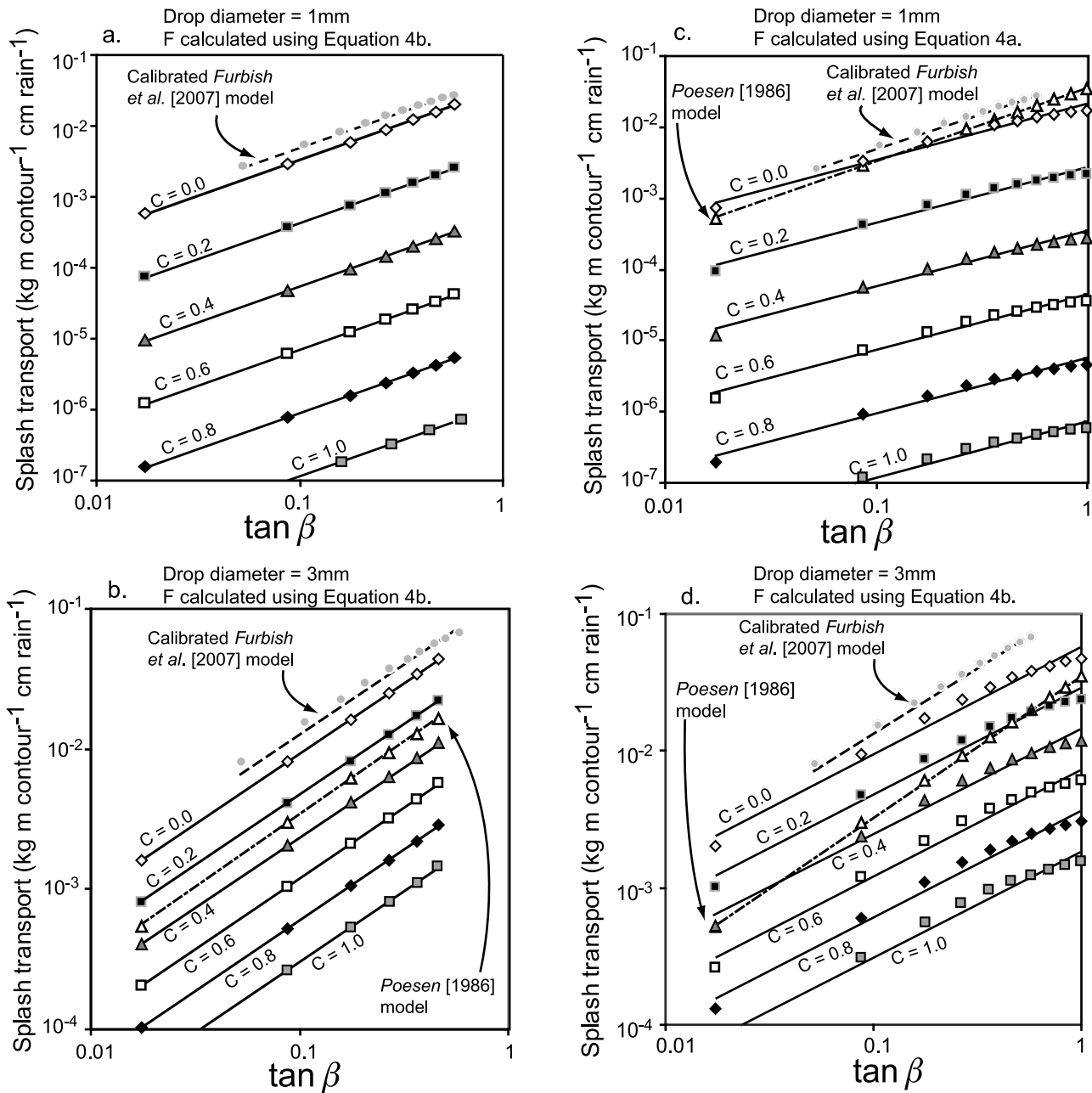


Figure 10. Values of splash transport per centimeter of rain from equation (14) for various values of hillslope angle β and cover density (C) for drop sizes of 1 mm and 3 mm with the linear estimation of F in equation (4b) and with the exponential estimation of F in equation (4a). The ejection angle, α_0 , was chosen to be 10° . When the linear estimate of F is used over the range $\beta < 25^\circ$, equation (14) closely approximates a linear relation between transport and $\tan \beta$. When the exponential estimate of F is used over the range $\beta < 45^\circ$, transport increases with $\tan^{0.78} \beta$, but deviates progressively from this simple form as gradient increases as indicated by the separation between the calculated points and the regressed power function. The graphs also show the sensitivity of transport to cover density, C ; it is greater for the 1 mm drops. The transport calculation from the model of *Furbish et al.* [2007], calibrated for a particle size of 0.2 mm, is also shown for bare soil with two drops sizes, and the prediction of *Poesen* [1985] for a bare loam soil is shown, except for Figure 10a in which Poesen’s curve is not distinguishable from our own.

slope on the alongslope partitioning of momentum and mass transport that creates a nonlinearity in the transport function. The nonlinearity increases as the range of slopes increases. However, as most hillslope angles with sparse vegetation and a soil cover fine enough to be splashed are

$< 25^\circ$, the linear relationship is a very close approximation of natural conditions.

[41] Takeoff angle, α_0 , remains in equation (14), and must be chosen on the basis of laboratory experiments. This angle may be related to grain size. However, it occurs both in the

integral and in the denominator of the coefficient in equation (14) and thus has offsetting effects on flux rate and the exponent b in equation (2). As particle size increases from 0.1 to 0.2 mm to 0.4 mm, the sparse data in Figure 9b suggest that α_0 might increase from 10° to as much as 47° , which reduces the flux in equation (14) by $\sim 50\%$, if the linear estimate of F is used.

[42] Only a few comparisons can be made of this equation with independent measurements from other sites with bare soil. *Poesen* [1986] published a summary of his own and other splash measurements, finding that the field measurements on bare tilled soil, bare patches of forest soils, and unpaved roads agreed well his transport equation. This equation, added as a dashed line to Figure 10, agrees almost exactly with our equation for a 1 mm raindrop and predicts 40% of our value for a 3 mm drop, if we use a bare soil with a detachability value (mass splashed per unit of rainfall kinetic energy) of $0.000588 \text{ kg J}^{-1}$ for a “loamy soil” from measurements by *Poesen and Savat* [1981] and kinetic energy values for these drop sizes from our own rainfall simulator.

[43] We have also calibrated the *Furbish et al.* [2007] model for comparison with equation (14). Rather than a fall line, the *Furbish et al.* [2007] model describes sediment ejection after drop impact as a probability distribution that is a function of the radial distance and angle about the center of impact. Two parameters must be calibrated in this model. The first is λ in equation (5) above, which describes partitioning of momentum between radial and downslope components. Using data compiled from *Poesen* [1985] and *Furbish et al.* [2007], we found λ to be 1.25 for $\beta < 25^\circ$. The second parameter, μ_0 , describes the mean distance traveled by ejected sediment. *Furbish et al.* [2007] found that μ_0 varied from 2 to 4 cm for drops between 2 and 4 mm and sediment particles between 0.35 and 0.85 mm.

[44] After determining the mass splashed by individual raindrops we transformed the probability distributions predicted by *Furbish et al.* [2007] into mass splashed across a unit length of contour. The mass splashed per drop has been observed by a number of authors to be a function of the drop momentum [e.g., *McCarthy*, 1980; *Mouzai and Bouhadef*, 2003; *Furbish et al.*, 2007]. We calculated the relationship between drop momentum, v ($\text{kg m}^{-1} \text{ s}^{-1}$), and mass splashed per drop, m (kg), for various particle sizes ($0.2 < d < 3.0 \text{ mm}$) based on *McCarthy's* [1980] experiments:

$$m = 0.14vd^{0.7} \quad (15)$$

for $v > v_{crit} = 4.08 \times 10^{-5}d^{1.37}$ where v_{crit} is the critical drop momentum required for splashing of a given particle size (see Figure 6). Unfortunately the raw data for individual splashes are not available from *McCarthy* [1980] for computing the precision of equation (15).

[45] The *Furbish et al.* [2007] model (equations (4), (7), and (8)) predicts a greater mass splashed than is predicted by equation (3) for bare soil if laboratory values of μ_0 are used. We suspect that microtopography on bare natural surfaces reduces mean splash distance relative to controlled laboratory experiments. To calibrate for field conditions, we reduced μ_0 values until the *Furbish et al.* [2007] model reproduced the mass splashed across a contour predicted by equation (3). We performed this calculation using values of mass splashed per

raindrop for 0.2 mm sediment particles. The calibrated values of μ_0 ranged between 0.67 and 1 cm. The fluxes then predicted by the *Furbish et al.* [2007] model exceed those of equation (14) by 43% in the case of 1 mm raindrops and by 33% in the case of 3 mm raindrops. This discrepancy is small compared to both cover and drop size effects (Figure 10).

[46] Thus, it appears that our rain splash transport equation (14), calibrated with splash measurements on an African grassland, which although grazed is not tilled or smoothed, results in flux predictions that overlap the range of bare tilled soils and bare patches of forest soils as well as prediction equations derived from single grain size laboratory experiments. Equation (14) also quantifies the role of raindrop size and ground cover density, which are both ultimately related to climate.

9. Discussion of Results

9.1. Role of Gradient

[47] Rain splash transport for a single rainstorm can be summarized in the form

$$q_{storm} = pq_{inst} = pk \tan^b \beta \quad (16)$$

where q_{storm} (kg m^{-1}) is the net downslope aerial splash and creep transport in a rainstorm of depth p (cm) in the absence of runoff. The exponent, $b = 1.0$ for slopes $< 25^\circ$ or $b = 0.78$ over the full range of gradient, reflects the form of the slope-dependent bracketed function in equation (14), which includes the hillslope gradient and the takeoff angle (a soil property). The slope function thus confirms the linear function used by *Kirkby* [1971] for modeling equilibrium hillslope profiles, and calculated by *McCarthy* [1980] and *Furbish et al.* [2007] from laboratory results. The 0.78 value is essentially the same as the value of 0.75 proposed by *De Ploey and Savat* [1968], but the nonlinearity only becomes relevant on gradients steep enough to maintain a soil cover that is either gravel-rich or stabilized by dense vegetation. The coefficient k in equation (16) combines the environmental controls: median drop size, vegetation cover, and soil mobility, and has a much larger effect on calculations of splash transport and hillslope profile evolution than does the exponent on gradient.

9.2. Role of Factors Related to Climate

[48] Equations (14) and (16) illustrate how rain splash is controlled by two climatic factors (drop size, D and rainstorm depth, p) and a biotic factor (C), which varies with the sum of all p values that yield the annual rainfall, possibly with season, and with grazing pressure. The influence on splash of p is linear for a single storm, though the number of these increments of rainfall depth and their average drop size over the entire rainfall climate is still required to compute $\rho_b K$ when the flux from equation (14) is inserted into the annual transport equation (2). The effect of the median drop size, D , will vary between storms, depending mainly on rainfall intensity, so that the equation will have to be integrated over the probability distributions of rainstorm intensity and duration in a climate to obtain the long-term value of $\rho_b K$. The effectiveness of ground cover density depends on the median drop size (equation (3) and Figure 4), being far more effective

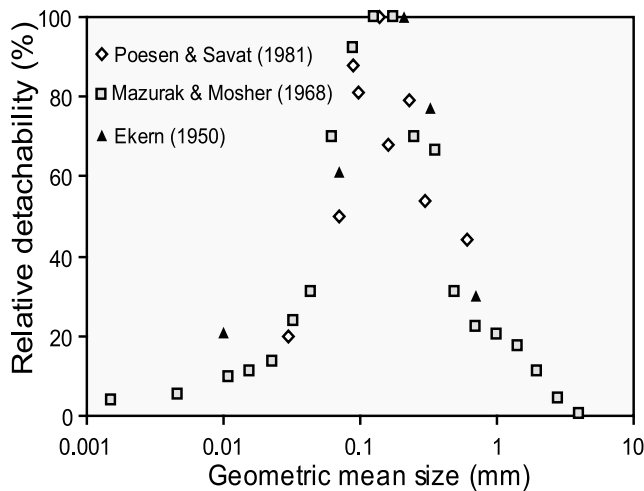


Figure 11. Detachability per unit of rainfall measured relative to the detachability of the most mobile texture class, which was set to 100% in each set of experiments. Symbols indicate the sources of each data set referred to in the text.

in reducing splash for small raindrops than for larger ones. This effect can be also seen in Figure 10, in which splash decreases with increasing cover much more rapidly for the smaller raindrop size. The exponential decline of transport with increasing cover is stronger than the commonly assumed linear effect of $(1 - C)$, presumably because the planform vegetation cover reduces impact while the associated density of erect stems or vegetation patches reduces lateral splash distances.

9.3. Role of Soil Characteristics

[49] The experiments used to parameterize equation (14) were conducted on a single soil type. It is interesting to estimate how much difference a change of texture might have on the soil mobility. Other soil characteristics have been used to explain and predict detachability, especially for cultivated soils that have been plowed and repacked, including shear strength, soil structure, organic content, and cation exchange capacity [Woodburn, 1948; Wischmeier *et al.*, 1971; Al-Durrah and Bradford, 1982]. However, the most widely available soil characteristic for unplowed, wildland soils is texture. The detachability of loose, repacked soils with a range of texture has been measured under laboratory rainfall simulators by Ekern [1950], Mazurak and Mosher [1968], and Poesen and Savat [1981]. We have plotted the results as detachability relative to that of the most detachable soil used for the particular experiments (Figure 11). The three sets of data show remarkable consistency with the most detachable soils having a median grain size of $0.125 < d_{50} < 0.21$ mm (fine sand), which includes the texture in our study, and with detachability declining strongly in both directions away from this maximum. Farmer [1973] used a slightly different metric to measure the relative detachability between grain size fractions of the same soil, and found a peak in relative detachability in the 0.4–0.5 mm range. Figure 11 suggests that the rain splash mobility values for other soils vary between about 5% and 100% of the value computed in this study. We are ignoring for the present purpose the role of

chemically active clays, bacterial coatings, and possible effects of other seasonal characteristics.

10. Spatial and Temporal Applicability of the Transport Equation

[50] Equation (14) accounts for aerial splash and creep transport in the absence of a surface water film, and thus it is applicable to an entire landscape during the parts of rainstorms that do not exceed the soil's infiltration capacity. At the site of the field study, for example, final constant infiltration capacity of the sandy clay loam ranges from about 1 to at least 8 cm h^{-1} , depending on rainfall intensity and local cover density [Dunne *et al.*, 1991, Figure 5]. The transient infiltration capacity earlier in the storm is several cm h^{-1} higher. If it is assumed, on the basis of our measured infiltration capacity curves [e.g., Dunne and Dietrich, 1980a], that storms up to 15 min long generate no significant surface water accumulation, then rainfall intensities for stations throughout Kenya, tabulated by Lawes [1974], indicate that in a climate with annual rainfall of about 22 cm in the period of record (Lodwar, NW Kenya), where the spatially averaged basal ground cover, C , is ~ 0.05 – 0.10 (based on quadrat measurements of ground cover by technicians of the Kenya Rangeland Ecological Monitoring Unit, compiled by Dunne [1981]), $\sim 60\%$ (14 cm) of the rain falls without generating surface runoff. This is equivalent to ~ 0.13 – $0.16 \text{ kg m}^{-1} \text{ a}^{-1}$ of soil transport by a median drop size of 2.5 mm on a 10° slope (assuming a takeoff angle of 10° for a sandy clay loam and the linear estimate of F). Basal cover is the most appropriate value to use for C because we have measured under experimental conditions [Dunne, 1977] that almost all of each season's rainfall occurs before the ground cover begins to expand. In a climate with ~ 80 cm of rain and $C = 0.35$ for the basal ground cover on grassland (Malindi, SE Kenya), about 40% of the annual rainfall would occur without generating runoff; the corresponding rates of splash would be $0.10 \text{ kg m}^{-1} \text{ a}^{-1}$. At the Amboseli study site (average basal $C = 0.1$) ~ 22 cm out of 27.5 cm occur without producing runoff. This amount would splash $0.20 \text{ kg m}^{-1} \text{ a}^{-1}$. Thus, equation (14) is applicable to a large fraction of the rainfall at any site.

[51] When it occurs, the process called “rain flow transport” by Moss *et al.* [1979] or “interrill erosion” by Meyer *et al.* [1975] is much more efficient than rain splash. However, rain splash is more widespread and frequent than rain flow transport on lightly disturbed landscapes where infiltration capacity remains relatively high and overland flow is rare. The splash transport rates predicted above for Lodwar (0.13 – $0.16 \text{ kg m}^{-1} \text{ a}^{-1}$), Malindi ($0.10 \text{ kg m}^{-1} \text{ a}^{-1}$), and Amboseli ($0.20 \text{ kg m}^{-1} \text{ a}^{-1}$) could lower hillslopes of 100 m length and 10° angles by 0.7 – $1.3 \times 10^{-3} \text{ mm a}^{-1}$. Dunne *et al.* [1979] estimated landscape-averaged erosion rates for various periods of the Cenozoic era at 8 – $30 \times 10^{-3} \text{ mm a}^{-1}$, indicating that rain splash transport alone cannot lower entire landscapes, even in the presence of preanthropogenic vegetation covers and infiltration capacities. On the other hand, 10 m long hillslopes could be eroded at 7 – $13 \times 10^{-3} \text{ mm a}^{-1}$, and 1 m long planes of typical “interrill” microtopography [Dunne *et al.*, 1995] could be eroded at ~ 70 – $130 \times 10^{-3} \text{ mm a}^{-1}$, if the splashed soil from

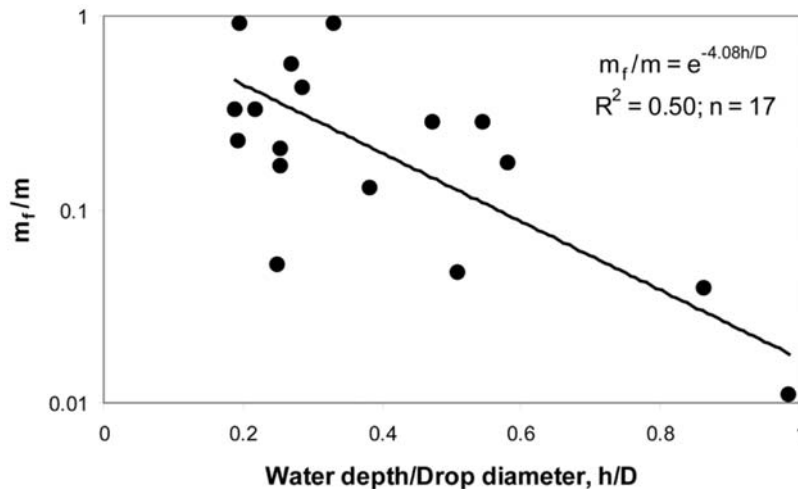


Figure 12. Variation of the ratio of mass splashed in the presence of a water film, m_f , to the mass splashed from bare, moist sand, m , with the ratio of water film depth, h , to raindrop diameter, D . Data are for single-drop impacts measured by McCarthy [1980].

their ends is carried away by runoff. This comparison with long-term erosion rates indicates that the morphogenetic role of rain splash acting alone is limited to parts of the landscape that lower more slowly than the landscape average, or to short hillslopes (<100 m) from which rain splash feeds soil to overland flow in the process of rain flow transport. Rain splash also tends to fill the rills initiated by overland flow, thereby suppressing channel formation, and maintaining smooth hillslope surfaces [Dunne and Aubry, 1985].

[52] Much of the landscape, however, is still affected by rain splash. Even during overland flow, the runoff depth, which is usually parameterized as a sheet with an average, “hydraulically effective,” depth for the purpose of runoff routing, varies from zero at the hillslope divide and at the top of microtopographic promontories [Dunne and Aubry, 1985]. The rate at which the average depth increases with distance along the slope depends on the runoff rate, local gradient, and flow resistance, which in turn depend mainly upon the ground cover density and microtopographic amplitude. Dunne and Dietrich [1980b] presented examples of the variability of runoff depths along contours on experimental plots at the Amboseli study site. Average flow depth increased with the square root of distance downslope, but at the high rates of runoff during the experiments, and on the low-gradient hillslopes characteristic of a craton, few zero depths were measured at the scale of the 5×2.5 m plots. However, further downslope on the same hillslopes the microtopography contains sufficient large-scale elements [Dunne et al., 1995] that runoff depths scaled by the hillslope length would not inundate a considerable fraction of the surface. Instead, this fraction would have only thin, discontinuous films of runoff, <1 mm deep, generated on local protuberances. On much steeper and rougher hillslopes in regions of more intense recent tectonism and climatic change and lower grazing and trampling pressure, Abrahams et al. [1989] showed that flow depths exhibited an exponential distribution, while Gabet and Dunne [2003] found a Poisson distribution; both cases indicating considerable areas of the hillslope microtopography with 0–1 mm scale water depths where splash should be only slightly affected by the water film.

[53] Palmer [1963, 1965] measured raindrop impact forces and splashed amounts of laboratory soil at low impact speeds, and concluded that as the thickness of a surface water layer increases so does splash erosion because of turbulence created in the water film, at least up to a water depth equal to the drop diameter. Wang and Wenzel [1970] challenged the identification of this maximum on the basis of better measurements and a numerical model of drop impact forces on the substrate. Whether or not a nonzero depth threshold exists, beyond some critical water depth splash detachment decreases exponentially as more of the drop energy is dissipated in the water film and the ejection angle (α_0) increases strongly to a value greater than 45° . Palmer estimated that the critical depth was approximately equal to D , and that the amount splashed was negligible for $h \geq 3D$. Torri and Sfalanga [1986] found the critical depth to be no more than $h = 0.2D$ for soil splash; and Mutchler and Young [1975] found it to be about $h = 0.14–0.2D$ for water splash. McCarthy’s [1980] measurements (Figure 12) indicate a strong decrease in mass of sand splashed into motion in the presence of a water film (m_f) as the ratio of water depth, h , to drop diameter, D , increases from zero to 1.0:

$$m_f = me^{-4\frac{h}{D}} \quad (17)$$

where m was the mass splashed without a water film, as in equation (13). The data are sparse and variable, but indicate a strong decline in the ratio of splash on a moist surface as a water film develops, suggesting the need for refinement of the relationship. Torri et al. [1987] found the coefficient in this exponent to be -0.9 for a sandy loam and larger for more cohesive soils. These results suggest that any critical depth can be ignored and that splash amounts decline to less than a tenth of their zero-depth values where flow depths exceed 0.6–1.0 times the drop diameter. Sample calculations, using values from literature referred to in the previous paragraph, indicate that several tenths of a runoff-generating surface are subject to identifiable rates of rain splash transport even during overland flow. Refinement of these estimates requires

more extensive sampling of rain splash and of the detailed spatial distribution of runoff depths on natural hillslopes.

11. Summary

[54] A goal of hillslope geomorphology has been to formulate sediment transport equations for individual sediment transport processes with sufficient physical resolution to identify major controls, the form of the equation, and the magnitude of its parameters. The research reported here provides such an equation. The functional form relating transport to hillslope gradient was shown to be linear over the range of gradients found on sparsely vegetated, soil covered hillslopes, and we have demonstrated that the momentum-partitioning approach to predicting this functional form [Furbish et al., 2007], can be calibrated to provide accurate transport values for bare soil. The magnitude of splash for a given gradient depends strongly on the climatically determined variables of rainstorm size, raindrop size, and cover density. We also summarized results from other researchers on the magnitude of the soil texture effect on splash. An analysis of the spatial and temporal significance of splash transport for a semiarid savanna suggests that rain splash mobilizes sediment on a large proportion of the landscape, either as aerial transport or as rain flow transport, but by itself has morphogenetic significance only on short hillslopes.

[55] However, even for rain splash, the simplest of all geomorphic processes, the construction of a physically based transport equation is fraught with complexity and the need to develop the equation with theory and with measurements from the laboratory and the field. The mechanics of splash leading to ejection angles (α_0) and the asymmetry of the upslope-downslope partitioning of sediment (F) remain poorly understood, but the momentum-partitioning approach of Furbish et al. [2007] appears to be the most promising theoretical approach to partitioning the splashed mass upslope and downslope, if it can be tractably extended to multidrop rainstorms and mixed grain size soils. It is not securely known whether soil grain size affects the ejection angle; nor has there been any thorough exploration of the effects of drop size on this angle. Detachability remains to be explored further, especially on cohesive soils and undisturbed soils that have not been dispersed and repacked for laboratory studies. On the other hand, scaling up of the equation to natural hillslopes, which bedevils studies of some other transport processes on hillslopes and in rivers, is not much of a problem, except for the need to know the spatial distribution of water depths during runoff generating storms.

[56] **Acknowledgments.** The work was supported by a grant from NSF Earth Science with logistical support from the Kenya Rangeland Ecological Monitoring Unit. Brian Aubry and Suzanne Fouty assisted with the field experiments and David Western provided information on local ecological conditions and processes. Conrad McCarthy stimulated the senior author's interest in defining the environmental conditions represented in rain splash transport equations. Suggestions from Joel Johnson and three anonymous reviewers improved the manuscript.

References

Abrahams, A. D., A. J. Parsons, and S. H. Luk (1989), Distribution of depth of overland flow on desert hillslopes and implications for modeling soil erosion, *J. Hydrol.*, *106*, 177–184, doi:10.1016/0022-1694(89)90173-X.

- Ahnert, F. (1976), Brief description of a comprehensive three-dimensional process-response model of landform development, *Z. Geomorphol., Suppl.*, *25*, 29–49.
- Ahnert, F. (1987), Process-response models of denudation at different spatial scales, *Catena Suppl.*, *10*, 31–50.
- Al-Durrah, M. M., and J. M. Bradford (1982), The mechanism of rain splash on soil surfaces, *Soil Sci. Soc. Am. J.*, *46*, 1086–1090.
- Carter, C. E., J. D. Greer, H. J. Braud, and J. M. Floyd (1974), Raindrop characteristics in the south central United States, *Trans. ASAE*, *17*(6), 1033–1037.
- Culling, W. E. H. (1960), Analytical theory of erosion, *J. Geol.*, *68*, 336–344, doi:10.1086/626663.
- De Ploey, J., and J. Savat (1968), Contribution a l'étude de l'érosion par le splash, *Z. Geomorphol.*, *12*, 174–193.
- Dietrich, W. E., D. Bellugi, A. M. Heimsath, J. J. Roering, L. Sklar, and J. D. Stock (2003), Geomorphic transport laws for predicting the form and evolution of landscapes, in *Prediction in Geomorphology*, *Geophys. Monogr. Ser.*, vol. 135, edited by P. Wilcock and R. Iverson, pp. 103–132, AGU, Washington D. C.
- Dunne, T. (1977), Intensity and controls of soil erosion in Kajiado District, Kenya, *Rep. Kenya Wildlife Manage. Proj.*, 67 pp., U.N. Food and Agric. Organ, Rome.
- Dunne, T. (1981), Effect of woodfuel harvest on soil erosion in Kenya, report, Beijer Inst. and Kenya Minist. of Energy, Nairobi.
- Dunne, T., and B. F. Aubry (1985), Evaluation of Horton's theory of sheetwash and rill erosion on the basis of field experiments, in *Hillslope Processes*, edited by A. D. Abrahams, pp. 31–53, Allen and Unwin, London.
- Dunne, T., and W. E. Dietrich (1980a), Experimental study of Horton overland flow on tropical hillslopes. Part I: Soil conditions, infiltration, and frequency of runoff, *Z. Geomorphol., Suppl.*, *33*, 40–59.
- Dunne, T., and W. E. Dietrich (1980b), Experimental study of Horton overland flow on tropical hillslopes. Part II: Sheetflow hydraulics and hillslope hydrographs, *Z. Geomorphol., Suppl.*, *33*, 60–80.
- Dunne, T., W. E. Dietrich, and M. J. Brunengo (1979), Rapid evaluation of soil erosion and soil lifespan in the grazing lands of Kenya, *IAHS AISH Publ.*, *128*, 421–428.
- Dunne, T., W. E. Dietrich, and M. J. Brunengo (1980), Simple, portable equipment for erosion experiments under artificial rainfall, *J. Agric. Eng. Res.*, *25*, 161–168, doi:10.1016/0021-8634(80)90057-8.
- Dunne, T., W. Zhang, and B. F. Aubry (1991), Effects of rainfall intensity, vegetation, and microtopography on infiltration and runoff, *Water Resour. Res.*, *27*, 2271–2285, doi:10.1029/91WR01585.
- Dunne, T., K. X. Whipple, and B. F. Aubry (1995), Microtopography of hillslopes and the initiation of channels by Horton overland flow, in *Evolving Concepts in Fluvial Geomorphology*, *Geophys. Monogr. Ser.*, vol. 89, edited by J. E. Costa et al., pp. 27–44, AGU, Washington D. C.
- Ekern, P. C. (1950), Raindrop impact as the force initiating soil erosion, *Soil Sci. Soc. Am. Proc.*, *15*, 7–10.
- Ekern, P. C., and R. J. Muckenhirn (1947), Water drop impact as a force in transporting sand, *Soil Sci. Soc. Am. Proc.*, *12*, 441–444.
- Ellison, W. D. (1944a), Two devices for measuring soil erosion, *Agric. Eng.*, *25*, 53–55.
- Ellison, W. D. (1944b), Studies of raindrop erosion, *Agric. Eng.*, *25*, 131–136.
- Ellison, W. D. (1948), Soil detachment by water in erosion processes, *Eos Trans. AGU*, *29*, 499–502.
- Farmer, E. E. (1973), Relative detachability of soil particles by simulated rainfall, *Soil Sci. Soc. Am. Proc.*, *37*, 629–633.
- Foster, G. R. (1982), Modeling the erosion process, in *Hydrologic Modeling of Small Watersheds*, edited by C. T. Han et al., pp. 297–380, Am. Soc. of Agric. Eng., Saint Joseph, Mich.
- Froehlich, W., and J. Slupik (1980), Importance of splash in erosion process within a small flysch catchment basin, *Stud. Geomorphol. Carpatho-Balcanica*, *14*, 77–112.
- Furbish, D. J., K. K. Hammer, M. Schmeckle, M. N. Borosund, and S. M. Mudd (2007), Rain splash of dry sand revealed by high-speed imaging and sticky paper splash targets, *J. Geophys. Res.*, *112*, F01001, doi:10.1029/2006JF000498.
- Furbish, D. J., E. M. Childs, P. K. Haff, and M. W. Schmeckle (2009), Rain splash of soil grains as a stochastic advection-dispersion process, with implications for desert plant-soil interactions and land-surface evolution, *J. Geophys. Res.*, *114*, F00A03, doi:10.1029/2009JF001265.
- Gabet, E. J., and T. Dunne (2003), Soil detachment by rain power, *Water Resour. Res.*, *39*(1), 1002, doi:10.1029/2001WR000656.
- Gilley, J. E., and S. C. Finkner (1985), Estimating soil detachment caused by raindrop impact, *Trans. ASAE*, *28*, 140–145.
- Greig-Smith, P. (1983), *Quantitative Plant Ecology*, 3rd ed., 359 pp., Univ. of Calif. Press, Berkeley.
- Hirano, M. (1969), Slope form and upheaval of the Yoro Mountain Range, central Japan (in Japanese), *J. Geol. Soc. Jpn.*, *75*, 615–627.

- Imeson, A. C. (1977), Splash erosion, animal activity and sediment supply in a small, forested Luxembourg catchment, *Earth Surf. Processes*, 2, 153–160, doi:10.1002/esp.3290020207.
- Kirkby, M. J. (1971), Hillslope process: Response models based on the continuity equation, *Inst. Br. Geogr. Spec. Publ.*, 3, 15–30.
- Kirkby, M. J. (1985), A model for the evolution of regolith-mantled slopes, in *Models in Geomorphology*, edited by M. J. Woldenberg, pp. 213–237, Allen and Unwin, London.
- Kirkby, M. J. (1989), A model to estimate the impact of climatic change on hillslope and regolith form, *Catena*, 16, 321–341, doi:10.1016/0341-8162(89)90018-0.
- Kwaad, F. J. P. M. (1977), Measurements of rain splash erosion and the formation of colluvium beneath deciduous woodland in the Luxembourg Ardennes, *Earth Surf. Processes*, 2, 161–173, doi:10.1002/esp.3290020208.
- Lane, L. J., M. A. Nearing, J. M. Laflen, G. R. Foster, and M. H. Nichols (1992), Description of the US Department of Agriculture water erosion project (WEPP) model, in *Overland Flow: Hydraulics and Erosion Mechanics*, edited by A. J. Parsons and A. D. Abrahams, pp. 377–391, Chapman and Hall, New York.
- Laves, E. F. (1974), An analysis of short duration rainfall, *Tech. Memo.* 23, 43 pp., East Afr. Meteorol. Dep., Nairobi.
- Mazurak, A. P., and P. N. Mosher (1968), Detachment of soil particles in simulated rainfall, *Soil Sci. Soc. Am. Proc.*, 32, 716–719.
- McCarthy, C. J. (1980), Sediment transport by rain splash, Ph.D. dissertation, 215 pp., Dep. of Geol. Sci., Univ. of Wash., Seattle.
- Meyer, L. D., G. R. Foster, and M. J. M. Römken (1975), Origin of eroded soil from upland slopes, in *Present and Prospective Technology for Predicting Sediment Yields and Sources*, pp. 177–189, U.S. Dep. of Agric., Washington, D. C.
- Morgan, R. P. (1978), Field studies of rain splash erosion, *Earth Surf. Processes*, 3, 295–299, doi:10.1002/esp.3290030308.
- Mosley, M. P. (1973), Rain splash and the convexity of badland divides, *Z. Geomorphol., Suppl.*, 18, 10–25.
- Moss, A. J., P. H. Walker, and J. Hutka (1979), Raindrop stimulated transportation in shallow water flows: An experimental study, *Sediment. Geol.*, 22, 165–184, doi:10.1016/0037-0738(79)90051-4.
- Mouzai, L., and M. Bouhadef (2003), Water drop erosivity: Effects on soil splash, *J. Hydraul. Res.*, 42, 61–68.
- Mutchler, C. K., and R. A. Young (1975), Soil detachment by raindrops, in *Present Prospective Technology for Predicting Sediment Yields and Sources*, pp. 114–117, U.S. Dep. of Agric., Washington, D. C.
- Palmer, R. S. (1963), The influence of a thin water layer on waterdrop impact forces, *Int. Assoc. Sci. Hydrol. Publ.*, 65, 141–148.
- Palmer, R. S. (1965), Waterdrop impact forces, *Trans. ASAE*, 8, 69–70.
- Poesen, J. (1985), An improved splash transport model, *Z. Geomorphol.*, 29, 193–211.
- Poesen, J. (1986), Field measurement of splash erosion to validate a splash transport model, *Z. Geomorphol., Suppl.*, 58, 81–91.
- Poesen, J., and J. Savat (1981), Detachment and transportation of loose sediments by raindrop splash, part II: Detachability and transportability measurements, *Catena*, 8, 19–41, doi:10.1016/S0341-8162(81)80002-1.
- Reeve, I. J. (1982), A splash transport model and its application to geomorphic measurement, *Z. Geomorphol.*, 26, 55–71.
- Salles, C., J. Poesen, and G. Govers (2000), Statistical and physical analysis of soil detachment by raindrop impact: Rain erosivity indices and threshold indices, *Water Resour. Res.*, 36, 2721–2729, doi:10.1029/2000WR900024.
- Sreenivas, L., J. R. Johnston, and H. O. Hill (1947), Some relationships of vegetation and soil detachment in the erosion process, *Soil Sci. Soc. Am. Proc.*, 12, 471–474.
- Torri, D., and M. Sfalanga (1986), Some aspects of soil erosion modeling, in *Agricultural Nonpoint Source Pollution: Model Selection and Application*, edited by A. Giorgini and F. Zingales, pp. 161–171, Elsevier, Amsterdam.
- Torri, D., M. Sfalanga, and M. Del Sette (1987), Splash detachment: Runoff depth and soil cohesion, *Catena*, 14, 149–155, doi:10.1016/S0341-8162(87)80013-9.
- Tsukamoto, Y. (1966), Raindrops under forest canopies and splash erosion (in Japanese with English summary), *Bull. Exp. For. Tokyo Univ. Agric. Technol.*, 5, 65–77.
- Van Dijk, A. I. J. M., L. A. Bruijnzeel, and E. H. Eisma (2003), A methodology to study rain splash and wash processes under natural rainfall, *Hydrol. Processes*, 17, 153–167, doi:10.1002/hyp.1154.
- Wang, R. C., and H. G. Wenzel Jr. (1970), The mechanics of a drop after striking a stagnant water layer, *Rep.* 30, 130 pp., Univ. of Ill. Water Resour. Cent., Urbana.
- Willgoose, G., R. L. Bras, and I. Rodriguez-Iturbe (1991), A coupled channel network growth and hillslope evolution model: 1. Theory, *Water Resour. Res.*, 27, 1671–1684.
- Wischmeier, W. H., C. B. Johnson, and B. V. Cross (1971), A soil erodibility nomograph for farmland and construction sites, *J. Soil Water Conserv.*, 26, 189–193.
- Woodburn, R. (1948), The effect of structural condition on soil detachment by raindrop action, *Agric. Eng.*, 29, 154–156.
- Young, R. A., and J. L. Wiersma (1973), The role of raindrop impact in soil detachment and transport, *Water Resour. Res.*, 9, 1629–1630, doi:10.1029/WR009i006p01629.

T. Dunne, Donald Bren School of Environmental Science and Management, University of California, Santa Barbara, CA 93106 USA.

D. V. Malmom, U.S. Geological Survey, 345 Middlefield Rd., Menlo Park, CA 94025, USA.

S. M. Mudd, School of Geosciences, University of Edinburgh, Edinburgh EH8 9XP, UK.